Computers, Materials & Continua CMC, vol.65, no.1, pp.419-432, 2020

A Novel Design of Mechanical Switch for the High Overload Environment

Yu Wang[1], Chen Liu[1], Lei Wang[2] and Lihua Zhu[1, *]

Abstract: The internal structure of the inertial measurement unit (IMU) in active state is easily damaged in the high overload environment. So that the IMU is usually required to be powered within the disappearance of the high overload. In this paper, a mechanical switch is designed to enable the IMU based on the analysis of the impact of high overload on the power-supply circuit. In which, parameters of mechanical switch are determined through theoretical calculation and data analysis. The innovation of the proposed structure lies in that the mechanical switch is triggered through the high overload process and could provide a delay signal for the circuit. After all, the proposed switch is tested through mechanical simulation, impact test and practical test. The experimental results show that the designed mechanical switch can effectively and reliably provide the delay for the circuit and guarantee operation of the IMU under high overload.

Keywords: High overload environment, mechanical switch, power-supply circuit, circuit delayed closing, data analysis.

1 Introduction

The projectile calculates its attitudes and position with the angular velocities and accelerations from the equipped inertial measurement unit (IMU), and sends it to the control center to realize functions such as expanding range and precise guide. Generally, it is necessary for the engineers to collect the exterior ballistic data and sensor output of projectiles for research [Ma, Xu and Kong (2015)]. However, conventional sensors could barely withstand the high overload in the projectile launching. It is to say, if a projectile-borne IMU is enable before launch, it is easily damaged or even malfunctioned within high overload. It is essential to have the projectile-loaded IMU powered after the high-overload impact in operation [Li, Li and Lian (2016)]. To avoid the high overload impact and protect the sensor, the non-contact mechanical overload switch just excites its mechanical contact during the overloading process, and provides a signal for the power-supply circuit of the sensors, so as to delay the electrified process.

At present, the overload switches based on spring oscillators and micro-mechanical structures are mainly in use. On one hand, the former directly or indirectly changes the

[1] School of Mechanical Engineering, Nanjing University of Science and Technology, Nanjing, 210094, China.

[2] School of Computing and Information Technology, University of Wollongong, Wollongong, NSW 2522, Australia.

[*]Corresponding Author: Lihua Zhu. Email: zhulihua@njust.edu.cn.

Received: 06 April 2020; Accepted: 17 May 2020.

contact state of the switch to realize the contact switching, but the contact state is difficult to maintain after the changes, let alone the machining procedure is complicated. On the other hand, the micro-electro-mechanical structures of the inertial switch could hardly survive in the great impact, making it inapplicable for high overload circumstances. In view of this issue, Wang et al. [Wang and Zhou (2005)] introduced a mechanical acceleration switch, which is design to close at 20000 g, at the same time, avoid the interference with a ball to isolate the upper and lower electrical plates. However, this switch might be triggered and close by mistake when the projectile fast rotates. Lian et al. [Lian and Wang (2016)] proposed a mechanical acceleration switch for the 550~1000 g overload application. It has the distinction of self-lock in close that the switch can maintain the lock state even within the 40000 g reverse high overload when the projectile hits the target. But the structure is too complicated to use. Xi et al. [Xi, Kong, Nie et al. (2019)] also presented an acceleration-sensitive switch to stand overloads between 800 g to 2400 g. but it could hardly withstand as much impact in the projectile launching and is easily damaged. Besides, switches have been developed for various purpose and applications, some of them are of limited range, while others cannot withstand the high overload and impact in the projectile launch process due to the structural destruction.

In this paper, a mechanical overload switch has been developed to address the problems mentioned above. The switch is a pure mechanical structure, which can not only withstand high overload during launching, but also maintain connected afterwards. It is simple and of high reliability. The contribution of the proposed switch mainly lies in three aspects: (1) It is an insurance for the acceleration impact that could keep the switch leads connected; (2) It is sensitive to the acceleration impact in order to automatically trigger the switch and cut the leads under high overload; (3) The switch is able have itself reset after the impact of the high overload.

The paper is organized as follows. The overall scheme of the mechanical overload switch is given in Section 2. Then, the determination of the component parameters of the mechanical overload switch are present through theoretical calculation in Section 3. In Section 4, a simplified model of the mechanical overload switch with specified material is built and tested through mechanical simulation. After that, physical experiments with Machete hammer and launching projectile and the corresponding analysis are shown in Section 5. Section 6 concludes the paper.

2 Overall scheme

Essentially, it is a cutting process to trigger the mechanical overload switch, the cutting manner of the lead is the key of the design. In which, an innovative method that inserting a high-hardness cross-shaped blade as a contact part in the head of a cylindrical excitation component is adopted. Without changing the casing of the mechanical overload switch, the lead of any diameters is able get cut with appropriate blades, proper excitation components and matching mass blocks. Where, the spring plays the role of insurance and also functions to reset the mechanical overload switch. The structure of the mechanical overload switch is shown in Fig. 1.

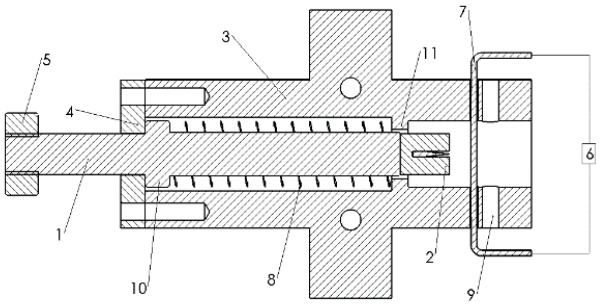

Figure 1: Structure of the mechanical overload switch

In Fig. 1, (1) is the mechanical overload switch excitation component. (2) is the contact. (3) is the overload switch casing. (4) is the overload switch casing cover. (5) is the mass block. (6) is the power supply circuit module. (7) is a switch lead, both of ends are connected to the external power supply module. The mechanical overload switch provides a signal to the external power supply module when (7) is cut by the excitation component [Cao, Wang and Bao (2016)]. (8) is a spring for supporting and resetting the excitation component to prevent false triggering and misconnection [Gerson, Schreiber and Grau (2014)]. (9) is used to fix the switch leads. (10) is a shoulder and (11) is a boss for supporting the spring.

The overall working procedures of the mechanical overload switch are given as follows.

Step 1. When the switch is in the off state. The mass block is threaded at the end of the excitation component and kept away from the contact.

Step 2. When it comes cross the overload impact, the mass block together with the excitation component compresses the spring in the switch casing, and resultant force is generated to cut the lead so as to turn on the switch.

Step 3. After the overload impact disappears, the restoring force of the spring sends the mass block and excitation component back to the original place, and the contact is kept away from the broken lead in order to avoid accidental contacts [Yang, Cai and Ding (2011)].

Besides, in Step 2, when the lead was cutting, the power supply module delayed the supply to the sensors and the data acquisition system, so that the acquisition system could function properly to record the sensor data [Huang, Gou and Li (2019)]. And in the whole process, it is very important to select an appropriate spring to avoid the false cutting due to the environmental interference.

3 Design of switch parameters

3.1 Design of the mechanical overload switch casing

Since the state of the lead determines whether the IMU is powered. The casing of the mechanical overload switch must be made of the insulating material with certain strength. Polyformaldehyde (POM) is an excellent engineering plastic with metal-similar hardness, strength and rigidity [Liang and Wang (2015)]. In view of its good self-lubricity, fatigue resistance, chemical resistance and wide-range flexibility, POM is able to adapt to the

harsh environment during the overload test, so that it has been selected to make the switch casing and the casing cover.

3.2 Design of excitation component and the mass block

The excitation component and the mass block are required be made of high-strength high-density materials. In this paper, the copper is chosen as the suitable metal material. As it is easy to obtain, not expensive, easily machined and unrusty [Jia (2018)]. The structural dimensions are designed using SOLIDWORKS, the total mass of the mass block and the excitation component is 12 g.

3.3 Design of the contact

During the interference and high overload test, the cylindrical excitation component rotates because of the acceleration wash inside the casing. If a single blade is used, the blade cannot keep perpendicular or intersected to the lead direction, resulting in failure of the mechanical overload switch under such conditions. In order to solve the problem, we have adopted an innovative crossing distribution of the blade, which reduces the requirement of contact installation, improves the reliability of the trigger, and the excitation component can be guaranteed to cut the lead in any angle when twisted.

Such material of blade is required with high-temperature hardness, high wear resistance, certain bending strength and impact toughness. Tungsten steel (hard alloy) has excellent properties such as high hardness, strength and toughness and heat resistance. It remains basically unchanged even under 500°C, and remains high hardness at 1000°C [Li (2016)]. Its high impact toughness, heat resistance could help to survive in harsh conditions of great overload. Therefore, in our design, the tungsten steel blade is mounted on the tip of the excitation component and is fixed by a high-strength, high-temperature resistant glue.

The specific structure diagram of the designed excitation component and contact is shown in Fig. 2.

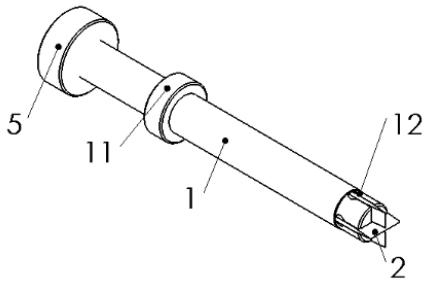

Figure 2: Structure diagram of excited component

Where, (1) is the copper excitation component. (2) is the contact, using an embedded cross-tungsten steel blade. (5) is the mass block. (11) is the excitation component shoulder. (12) is the cross recess of the excitation component for inserting the blade.

3.4 Design and data analysis of the Spring

The selection of the spring is the key of the design. According to Hooke's law, within the elastic limit, when the spring is elastically deformed, the spring force F of the spring is proportional to the elongation (or compression) x of the spring, that is $F = -k * x$. Where k is the elastic coefficient of the spring (or stiffness coefficient, strength coefficient) [Zi and Wu (2015)].

The spring in the mechanical switch functions in two aspects. One is the fuse function, which is used to support the excitation component and prevent accidental close under the interference impact. The other is the reset function. If the lead gets cut, the spring would reset the excitation component to prevent failure of switch that caused by the excitation component and the lead wire sticking.

For function one, the purpose is to prevent the mechanical switch from being triggered by the disturbance acceleration during the transportation or falling.

The amplitude of the acceleration pulse caused by the falling is 10000-15000 g, the time of the acceleration pulse is about 100-300 μs [Chen (2014)]. g (gravitational acceleration) is 10 m/s^2. Assuming that the amplitude of the disturbance acceleration is 10000 g and the time is 100 μs [Nie, Zhou, Xi et al. (2017)]. The accidental falling acceleration pulse can be approximated by a half sinusoid [Yang, Ding, Wang et al. (2018)]. The acceleration pulse in the case of an accidental falling is shown in Fig. 3(a).

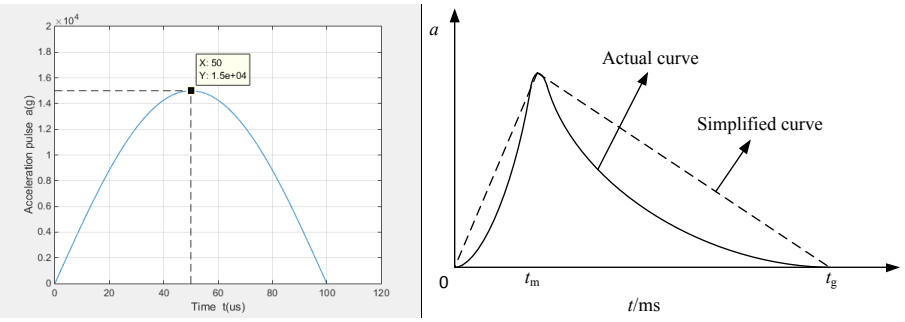

(a) Acceleration pulse in an accidental fall. (b) Curve of high overload acceleration

Figure 3: Acceleration pulse in different states

The initial velocity v_0 before impact can be obtained through integration of the half sinusoid. the curve integration could approximate to the product of one-third of the peak value and pulse time. The initial speed v_0 and the initial kinetic energy W_0 of the mechanical switch mass block and the excitation component in the accidental falling event can be described as follows:

$$v_0 = \frac{1}{3} \times 10000 \times 10 \times 0.0001 = 3.333 \tag{1}$$

$$W_0 = \frac{1}{2} \times 0.012 \times 3.333^2 = 0.0667 \tag{2}$$

The designed distance between the contact and the lead is 8 mm, that is, the spring

compression amount x_1 is up to 8 mm under the interference impact. The spring elastic potential energy W_{k0} is:

$$W_{k0} = \frac{1}{2} \times k \times \left(x_2 \right)^2 = 0.000032 \times k \tag{3}$$

In the context of disturbance acceleration, the kinetic energy of the mass block and the excitation component need be totally converted to the elastic potential energy of the spring, so that the mechanical switch would not get laid. Therefore, Eq. (4) needs to be satisfied:

$$0.000032 \times k \geq 0.0667 \tag{4}$$

It follows that the elastic coefficient of the spring needs to be greater than 2083 N/M.

For the reset function, it is to serve as the reliability insurance. The excitation component is reset to prevent the contact and the excitation component from contacting the disconnected lead, while the two ends of the lead are kept connected. To reset the excitation component after the overload impact, it only requires the spring's elastic potential energy being greater than the work of the mass block and the excitation component gravity. According to the above design, the spring compression amount x_1 has a minimum of 8 mm. After experiencing high overload, the work of overcoming gravity W_2 is calculated with Eq. (5).

$$W_2 = m_1 \times g \times x_2 = 0.00096 \tag{5}$$

The spring elastic potential energy W_1 (J) is given by:

$$W_1 = \frac{1}{2} \times k \times \left(x_2 \right)^2 = 0.000032 \times k \tag{6}$$

It is necessary to satisfy $W_1 \geq W_2$, that is, the elastic coefficient of the spring is $k \geq 30$ N/M.

In high overload circumstance, it is necessary consider the change of acceleration for the selection of the spring elastic coefficient. The overload acceleration curve is shown with the solid line in Fig. 3(b). And the simplified acceleration variation is given in Eq. (7).

$$\begin{cases} a = \dfrac{p_1 g}{t_m} t & 0 \leq t \leq t_m \\ a = \dfrac{p_2 g \left(t_g - t \right)}{t_g - t_m} t & t_m \leq t \leq t_g \end{cases} \tag{7}$$

where, p_1 is the maximum overload impact coefficient, t_m is the time for the projectile to achieve maximum acceleration in chamber, t_g is the time for the projectile reaching the muzzle [Zhou, Zhang and Lian (2015)]. The specified overload characteristics are a_1=15000 g, t_m=3 ms, t_g=10 ms, that is, the maximum acceleration of 15000 g happened in 3 ms. When t=t_m, the overload reaches the threshold. Then, p_1 can be computed from Eq. (8).

$$p_1 = 15000 \times g \times 0.003 \div g \div 0.003 = 15000 \tag{8}$$

In is demanded that the mechanical overload switch can be triggered properly in the overload test, the safety threshold is set to 500 g. It is, the designed overload index of mechanical overload switch is 14500 g, and it can be calculated that t=2.9 ms. In other word, the designed overload index of mechanical overload switch is standard in 2.9 ms

after overload impact happens.

From the curve of high overload acceleration in Fig. 3(b), the centroid acceleration of the total mass of the mass block and the excitation component is linear. If the lead is contacted after period t_1, the centroid movement distance and the spring compression amount are equally x_3=8 mm. Then, the acceleration of the centroid can be expressed by the average acceleration a_3 during the process, and the work done by the centroid motion W_3 (gravity work and friction work can be neglected here) must be greater than the elastic potential energy W_4 after the spring is compressed.

$$W_3 = m_1 \times a_3 \times x_3 = m_1 \times \frac{\frac{p_1 g}{t_m} \times t_1}{2} \times x_3 = 2400 \times t_1 \tag{9}$$

$$W_4 = \frac{1}{2} \times k \times (x_3)^2 = 0.000032 \times k \tag{10}$$

The time for the overload to reach the designed threshold of the mechanical overload switch is 2.9 ms, and the time required for the contacting the leads is t_1=0.9 ms. At 0.9 ms, $W_3 \geq W_4$, that is $k \leq 67500$ N/M.

From the above analysis, the selection range of spring's elastic coefficient is $2083 \leq k \leq 67500$ N/M. In this paper, the elastic coefficient k is set to 2200 N/M. Based on the determined elastic coefficient and practical needs, the spring parameters can be determined that the wire diameter is 1mm, the outer diameter is 8mm, the total number of coils is 15, the height is 35 mm, the material is 65 Mn spring steel. The total mass of the excitation component and the mass block is 12 g. The contact is made of tungsten steel blade, which is embedded in the cross section on the excitation component. The contact is 8mm away from the edge of the lead. The mechanical overload switch casing and casing cover is made of POM insulation material.

4 Mechanical analysis on the spring

It is necessary to conduct experiments on mechanical overload switch before trial to find out the design deficiencies and make improvement as much as possible [Sun (2015)]. Since the spring plays a key role in the mechanical overload switch. The impact of the overload acceleration on the excitation component, the mass block and the contact can be reflected indirectly by the compression of the spring. Therefore, the equivalent model of spring should be established to simulate the overload impact on the leads.

To simplify the mechanical switch model, the work done by the excited part and mass block can be simplified to the work done by mass block on the spring under acceleration impact. At the same time, the elastic coefficient of the selected spring can be analyzed by the compression extent of the spring. The established equivalent model of spring through finite element is shown in Fig. 4.

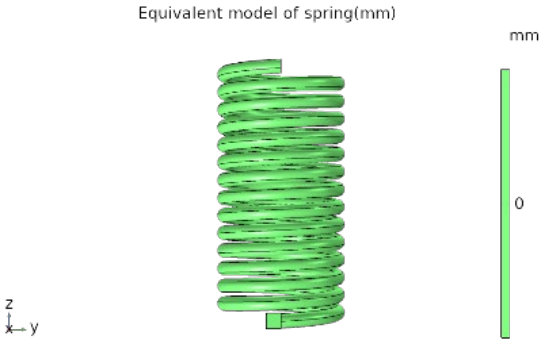

Figure 4: Equivalent model of spring

The compression amount of the spring under acceleration impact can be approximated by the displacement of the mass block. The equivalent model of spring with disturbance acceleration is shown in Fig. 5(a). The equivalent model of spring at the overload peak is shown in Fig. 5(b).

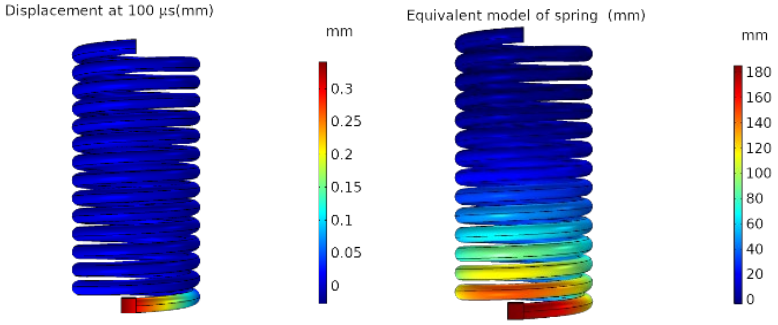

(a) Interference state (b) Overload peak state

Figure 5: Equivalent model of spring under different states

The displacement diagram of the mass block with the disturbance acceleration is shown in Fig. 6(a). The displacement diagram of the mass block under the high overload acceleration is shown in Fig. 6(b).

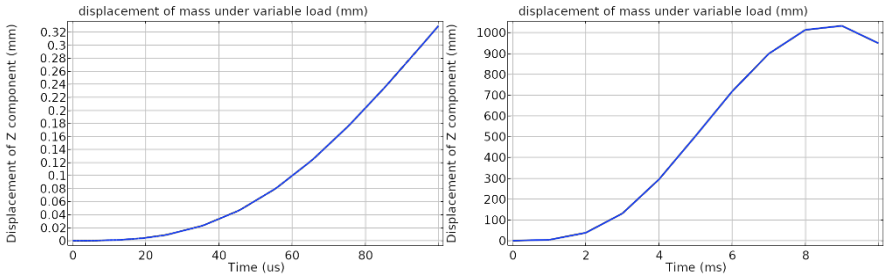

(a) Within disturbance acceleration (b) Within high overload acceleration

Figure 6: Mass displacement within different acceleration

As it is seen from Fig. 6(a), the compression amount of the spring under the disturbance acceleration (10000 g, t_m=100 μs) was 0.3 mm and the compression amount at the overload peak (15000 g, t_m=3 ms) was 166 mm.

Because the impact time of the disturbance acceleration is extremely short, the compression amount of the spring is much less than 8 mm, which confirms that the mechanical overload switch did not close under the disturbance acceleration.

In the high overload peak test, the spring compression is much larger than the contact-to-lead distance and the lead diameter (2 mm), indicating that the excitation component and the mass block can compress the spring to the lead edge under the overload impact acceleration, and convert the remaining energy of acceleration impact to cut the leads.

It is seen that the mechanical overload switch structure of the above design is reasonable and can function reliably in the process of high overload through mechanical simulation and stress analysis. The physical picture of mechanical overload switch is shown in Fig. 7. The ends of the lead are used to connect the peripheral judgment circuit.

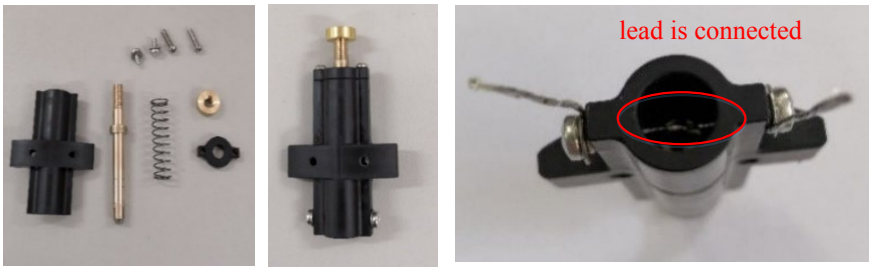

(a) Components of mechanical overload switch (b) Mechanical overload switch without lead (c) Mechanical overload switch with lead

Figure 7: Physical picture of mechanical overload switch

5 Experiments and tests

In order to verify the capability of the proposed design, the Machete hammer test and the launching projectile experiment were carried out. The detailed experimental analysis is given in subsections.

5.1 Machete hammer test

In the case of high overload impact, the Machete hammer test was performed on the mechanical overload switch to verify the influence of different diameter lead wires on the mechanical overload switch operation and the reliability of the component strength under the impact environment.

The Machete hammer test is a common method to test the reliability of overload fuses and the strength of components and other overload resistance. The Machete hammer test bench converts the gravitational potential energy of the test bench's weight into kinetic energy through gravity, and strikes the target to be tested, causing an overload impact. The amplitude of the acceleration pulse generated by the Machete hammer can reach up

to 40000g or more, but the duration of the force is short, and the general pulse width is about 120 μs [Lin, Zhang, Li et al. (2015)].

Tab.1 shows the correspondence between the number of teeth and the impact acceleration value of the Machete hammer test bench used in this experiment.

Table 1: Correspondence between the teeth number and the impact acceleration

Teeth number	Impact acceleration/*g*	Impact time/*us*
3	3671±152	106
7	5608±611	88
12	8297±337	75
15	13011±25	64
17	29 942±1368	48
20	43289±587	36

In the experiment, PTFE insulated silver-plated copper leads of different outer diameter were experimented in the Machete hammer test [Wang, Tian, Wang et al. (2019); Wang, Yang, Wang et al. (2020)]. The photo of the Machete hammer test bench is shown in Fig. 8.

Figure 8: Bench of Machete hammer test

For data analysis and comparison, two groups of springs, namely *Spring* 1 and *Spring* 2 separately, were tested on the Machete hammer bench. Both of two-groups springs are made of 65 Mn steel. The parameters of the two group springs are shown in Tab. 2.

Table 2: The parameter setting of *Spring* 1 and *Spring* 2

	Elastic coefficient k (N/M)	Wire diameter (mm)	Out diameter (mm)	Total coil number	Height(mm)
Spring 1	2200	1	8	15	35
Spring 2	2043	1	8	16	38

The experimental results of the two sets springs in Machete hammer test are shown in Tabs. 3 and 4.

Table 3: Relationship between the outer diameter of the wire and wire state of *Spring* 1

Test order	Experiment times	Out diameter of leads (mm)	Teeth of Machete hammer	Lead cut
1	5	0.7	15	Yes
2	5	0.87	15	Yes
3	5	0.98	15	Yes
4	5	1.18	15	Yes
5	2	1.28	15	No
6	2	1.28	17	Yes
7	2	1.4	15	No
8	2	1.4	17	Yes
9	5	1.18	12	No

According to the Machete hammer test, the switch can not only cut the high-temperature resistance lead with an outer diameter of 1.18 mm or less, but also reset the excitation component and the mass block after the overload impact acceleration disappears.

Table 4: Relationship between the outer diameter of the wire and wire state of *Spring* 2

Test order	Experiment times	Outer diameter of leads(mm)	Teeth of Machete hammer	Lead cut
1	5	0.7	12	Yes
2	5	0.87	12	Yes
3	5	0.98	12	Yes
4	5	1.18	12	Yes
5	5	1.28	12	Yes
6	2	1.4	12	No
7	2	1.18	15	Yes

It is seen from Tab. 4 that the switch with *Spring* 2 can cut the lead wire with an outer diameter of less than 1.28 mm when the interference acceleration impact reaches 8297±337 g, which means that the lead is unable to keep intact within the interference acceleration impact. On the contrary, it can be seen from Tab. 3 that the switch with *Spring* 1 who satisfy the experimental requirements of the elastic coefficient can not only

withstand the interference acceleration impact, but also automatically cut the lead during a high overload.

Combining the Machete hammer test, Tabs. 3 and 4, it can be drawn that, under the acceleration disturbance of 8297±337 g, the mechanical overload switch with *Spring* 1 and *Spring* 2 can cut the high temperature wire with the outer diameter less than 1.18 mm. Meanwhile, the *Spring* 1 switch could not cut the wire with outer diameter 1.18 mm. The *Spring* 2 switch could cut the wire with outer diameter of 1.28 mm. And under the acceleration impact 13011±25 g, the mechanical overload switch with *Spring* 1 and *Spring* 2 could cut the high temperature wire with outer diameter 1.18 mm. It demonstrated that when the spring's elastic coefficient satisfies 2083≤k≤67500N/M, the proposed mechanical overload switch can function accurately: keeping the switch lead connected under the interference acceleration impact, and cutting the lead under the stated impact.

5.2 Launching test

In this section, two groups of experiments with four mechanical overload switches are tested. In the experiment, the copper crusher gauge is employed to calculate the peak of the high overload. The obtained high overload peaks of the two groups are 15425 g and 16041 g respectively, and the overload durations t_g are 14 ms and 16 ms, respectively.

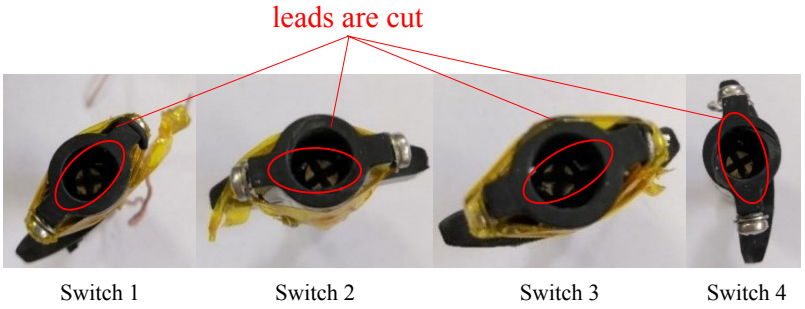

Figure 9: Physical pictures of experimented switches after launching

After the launching experiment, the projectile was retrieved. We checked the mechanical overload switches. The physical picture of the four tested mechanical overload switches are shown in Fig. 9. It is seen that the leads in the mechanical overload switches have been successfully cut, so that the lead is switched from on to off. Besides, we have collected the valid data of the external ballistic sensor, which means that the sensor works normally after experiencing a high overload process. At the same time, the excitation component has been reset. From the launching experiment, it is demonstrated the effectiveness of the proposed high overload switch.

6 Conclusion

Responding to the proper operation requirements of the IMU after high overload in the exterior ballistic test, a novel mechanical overload switch has been designed, which perfectly solves the problem using a non-contact switch to enable the IMU after the high

overloading process. The proposed mechanical switch has been verified through simulation and experimental. It helps to fulfill the out-chamber power-on of the IMU and data acquisition of the exterior trajectory. At the same time, the integrity of the mechanical overload switch after the high overload test confirmed its reusability and reliability. In case of the extending application in other use, a mechanical overload switch can be redesigned by selecting the proper spring and lead with specific overload magnitude.

Funding Statement: This work was supported by the National Natural Science Foundation of China (No. 61803203).

Conflicts of Interest: The authors declare that they have no conflicts of interest to report regarding the present study.

References:

Cao, S.; Wang, Y. S.; Bao, T. Y. (2016): A high reliability graze burst switch of electromechanical contact fuze. *Journal of Detection & Control*, vol. 38, no. 5, pp. 27-30.

Chen, J. J. (2014): *Design of Micro-Mechanical Inertial Blocking Switch* (*M.E. Thesis*). Nanjing University of Science and Technology, China.

Gerson, Y.; Schreiber, D.; Grau, H. (2014): Meso scale MEMS inertial switch fabricated using an electroplated metal-on-insulator process. *Journal of Micromechanics and Microengineering*, vol. 24, no. 2, pp. 1-8.

Huang, J. C.; Gou, L. P.; Li, X. F. (2019): Research on acceleration detection method of overload switch operation. *Electromechanical Component*, vol. 39, no. 2, pp. 48-50.

Jia, C. C. (2018): Metals (2): small secrets of metal density and melting point. *Metal World*, no. 3, pp. 26-30.

Li, L. X.; Li, B.; Lian, Y. F. (2016): Design of mechanical inertial acceleration switch. *Hebei Agricultural Machinery*, vol. 41, no. 3, pp. 46-48.

Li, W. H. (2016): *Synthesis, Characterization and Mechanical Properties Research of Novel Tungsten Steel Composite (M.E. Thesis)*. Beijing Institute of Technology, China.

Lian, Y. F.; Wang, L. (2016): Design of inertial acceleration switch for fuze. *Fire Control and Command Control*, vol. 41, no. 3, pp. 154-157.

Liang, J. Z.; Wang, F. (2015): Flexural and impact properties of POM/EVA/HDPE blends and POM/EVA/HDPE/ nano-CaCO3 composites. *Polymer Bulletin*, vol. 72, no. 4, pp. 915-929.

Lin, R.; Zhang, Z. H.; Li, K. J.; Zhang, D. H.; He, X. (2015): Review of high impact calibration technology of high G accelerometers. *Journal of Detection and Control*, vol. 37, no. 4, pp. 106-112.

Ma, Q. Q.; Xu, X. H.; Kong, Y. K. (2015): Anti-high overload analyses and design of missile-borne recorder. *Journal of Projectiles, Rockets, Missiles and Guidance*, vol. 35, no. 1, pp. 15-18.

Nie, W. R.; Zhou, Z. J.; Xi, Z. W.; Bu, C.; Luo, Q. (2017): A novel dual-threshold MEMS acceleration latching switch. *IEEE International Symposium on Inertial Sensors and Systems*, *Kauai*, *Hawaii*, *USA*, pp. 54-57.

Sun, J. L. (2015): *Design of Miniature High Reliability Overload Switch* (*M.E. Thesis*). Harbin Institute of Technology, China.

Wang, J.; Yang, Y. Q.; Wang, T.; Sherratt, R. S.; Zhang, J. Y. (2020): Big data service architecture: a survey. *Journal of Internet Technology*, vol. 21, no. 2, pp. 393-405.

Wang, L.; Zhou, B. L. (2005): A new inertial acceleration switch of mechanical pattern. *Journal of Gun Launch and Control*, no. 2, pp. 40-43.

Wang, Z. L.; Tian, N. C.; Wang, J. G.; Yang, S. Q.; Liu, G. (2019): Mechanical response and energy dissipation analysis of heat-treated granite under repeated impact loading. *Computers, Materials & Continua*, vol. 59, no. 1, pp. 275-296.

Xi, Z. W.; Kong, N.; Nie, W. R.; Cao, Y.; Zheng, C. (2019): High g MEMS inertial switch capable of direction detection. *Sensors and Actuators A: Physical*, vol. 296, pp. 7-16.

Yang, Z. Q.; Cai, H. G.; Ding, G. F. (2011): Dynamic simulation of a contact-enhanced MEMS inertial switch in Simulink. *Microsystem Technologies*, vol. 17, no. 8, pp. 1329-1342.

Yang, Z. Q.; Ding, G. F.; Wang, Y.; Zhao, X. L. (2018): A MEMS inertial switch based on non-silicon surface micromachining technology. *Micro Electro Mechanical Systems. Micro/Nano Technologies*, vol. 4, no. 1, pp. 945-995.

Zhou, X. S.; Zhang, Y.; Lian, Y. F. (2015): Design of mechanical inertial switch. *Mechanical Research & Application*, vol. 28, no. 6, pp. 95-100.

Zi, T. Y.; Wu, B. (2015): On the analysis and improvement of the demonstrative experiment of Hooke's Law in the old and new textbook of senior high schools. *Journal of Zunyi Normal College*, vol. 17, no. 6, pp. 140-144.